Separation Science and Technology
Publication details, including instructions for authors and subscription information:
http://www.informaworld.com/smpp/title~content=t713708471

Physico-Chemical Properties of Supported and Unsupported γ-Al_2-O_3 and TiO_2 Ceramic Membranes

M. J. Gieselmann[a]; M. A. Anderson[a]; M. D. Moosemiller[b]; C. G. Hill Jr.[b]
[a] Water Chemistry Program, University of Wisconsin, Madison, Wisconsin [b] Department of Chemical Engineering, University of Wisconsin, Madison, Wisconsin

To cite this Article Gieselmann, M. J. , Anderson, M. A. , Moosemiller, M. D. and Hill Jr., C. G.(1988) 'Physico-Chemical Properties of Supported and Unsupported γ-Al_2-O_3 and TiO_2 Ceramic Membranes', Separation Science and Technology, 23: 12, 1695 — 1714
To link to this Article: DOI: 10.1080/01496398808075658
URL: http://dx.doi.org/10.1080/01496398808075658

SEPARATION SCIENCE AND TECHNOLOGY, 23(12&13), pp. 1695-1714, 1988

PHYSICO-CHEMICAL PROPERTIES OF SUPPORTED AND UNSUPPORTED γ-Al_2O_3 AND TiO_2 CERAMIC MEMBRANES

M. J. Gieselmann
M. A. Anderson
Water Chemistry Program
University of Wisconsin
Madison, Wisconsin 53706

M. D. Moosemiller
C. G. Hill, Jr.[1]
Department of Chemical Engineering
University of Wisconsin
Madison, Wisconsin 53706

ABSTRACT

Supported and unsupported γ-Al_2O_3 and TiO_2 ceramic membranes have been prepared by sol-gel techniques from alkoxide precursors. Several physico-chemical properties of these materials have been determined. N_2 sorption analysis has been used to determine pore size distributions and mean pore sizes. Particle sizes of sols as measured by "in situ" quasi-elastic light scattering are discussed in the light of SEM analyses of the sintered membranes prepared from these sols. Crack-free unsupported monoliths of Al_2O_3 with thicknesses up to 100 μm have been prepared. Similarly, supported Al_2O_3 and TiO_2 membranes with thicknesses of 0.5 μm have been produced. Preliminary measurements of the permselectivities of supported membranes have also been made.

INTRODUCTION:

Over the past two decades membrane separation processes have been applied with increasing frequency to solve separation

[1] Author to whom correspondence should be addressed

problems. Industry has utilized such techniques as reverse osmosis, ultrafiltration, and electrodialysis to effect the concentration and fractionation of a wide variety of process fluids, both liquid and gas. Major advantages associated with the use of these processes include high permselectivities, low energy requirements relative to alternative separation techniques, and suitability for operation at low temperatures in processing such thermally labile materials as pharmaceuticals and foodstuffs. Throughout the time frame in question systems based on polymeric membranes have dominated the commercial market, but currently significant interest exists in developing ceramic based systems for industrial scale applications.

There are several potential advantages to the use of ceramic membranes, particularly with respect to their stability at high temperatures, in harsh chemical environments (e.g., in strong cleaning solutions or in the presence of organic solvents), and in the presence of microbes. Consequently a number of research groups, both in this country and abroad, are actively pursuing the task of developing permselective ceramic membranes. The present paper describes the results of some of our efforts to utilize sol-gel technology to prepare permselective ceramic membranes and to characterize some of their fundamental properties.

A variety of preparative methods has been used to fabricate both supported and unsupported ceramic membranes formed of TiO_2 and Al_2O_3 (1-11). Our research program is directed toward producing ceramic membranes of TiO_2 and γ-Al_2O_3 having a desired pore size, pore size distribution, and predictable surface properties by controlling the suspension and interfacial chemistries of the precursor sols. To this end our major objectives are: 1. to understand the major solution variables (pH, ionic strength, specific solute effects, etc.) controlling sol and gelation chemistries, since these sols and gels serve as precursors to ceramic membranes, and 2. to study the effects of these variables, as well as sintering conditions, on the properties of the final ceramic membranes (both supported and unsupported). Our earlier effort in this area (12) focused on how various preparation protocols influenced the tendency of the gels to form crack-free membranes. The present paper concerns the physico-chemical and permselective properties of membranes formed from TiO_2 and Al_2O_3.

MATERIALS AND METHODS:

Materials

Titanium tetraisopropoxide was obtained from Aldrich Chemical Company while aluminum tri-sec-butoxide was obtained from Alfa Chemical Company. Both ethyl alcohol (absolute) and isopropanol were AR grade. All chemicals were used without further purification. Water used in reactions was deionized using a Milli-Q water purification system (Millipore Corp.).

Table 1. Compositions of Clays Used to Prepare Membrane Supports (Weight Percentages)

Component	'OM-4' Ball Clay	'AP-Green' Fire Clay
SiO_2	55.6	55.23
Al_2O_3	28.6	38.11
TiO_2	1.8	2.05
Fe_2O_3	1.0	1.55
CaO	0.1	0.32
MgO	0.4	0.71
Na_2O	0.1	0.16
K_2O	1.1	1.45
Loss on Ignition	11.4	10.0
Bulk Density (g/cc)	0.62	1.26

Clays used in the preparation of membrane supports were obtained from Paoli Clay Company and had the compositions given in Table 1.

The polyethylene glycols used in the permselectivity studies were obtained from Aldrich Chemical Company. Their nominal molecular weights were 200, 1000, and 8,000. Another model system used in this phase of the research was a 98-99% pure bovine serum albumin with a molecular weight of 66,000 obtained from Sigma Chemical Company.

Methods for Production of Membranes

The TiO_2 and Al_2O_3 membranes were prepared using the sol-gel technique described in a previous paper (12). The experimental protocol is summarized in Figure 1. The indicated approaches yielded TiO_2 and γ-Al_2O_3 membranes from both particulate and polymeric $Ti(OH)_4$ sols and particulate γ-AlOOH sols.

Analytical Methods

Polyethylene glycol. Aqueous solutions of PEG were analyzed for concentration using a Nicolet Model 60SX Fourier transform infrared (FTIR) spectrometer equipped with a cylindrical internal reflectance cell. A useful peak was the C-O stretching band at 1080 to 1090 cm^{-1}. The difference between the absorbances at the peak and at the base line (as measured at 1200 to 1210 cm^{-1}) was linearly related to the concentration of PEG in the solution. However, the base line values changed from day to day on the instrument. Thus for each day that analyses were conducted, high and low concentration standards were tested for absorbance. The concentrations of the experimental samples were determined by interpolation between the standards.

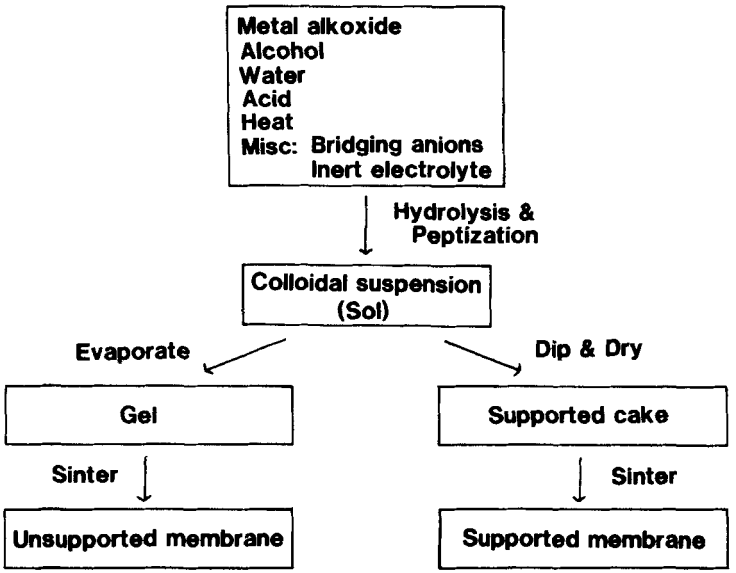

Figure 1. Preparation protocol.

Albumin. Concentrations of albumin in aqueous solution were determined by a total solids analysis.

Equipment. The apparatus used to determine the permselectivity characteristics of the ceramic membranes was a standard test loop which consisted of the following components: (see Figure 2): feed cylinder, LEWA positive displacement pump with outlet flow dampener, high pressure relief valve, 20.6 mm I.D. by 22 cm-long pressure cell, needle valve back pressure regulator (for high corrosion service), Tescom Model 26-3225-24 springloaded back pressure regulator (for low corrosion service), retentate flow rotameter, permeate collector, and copper tubing coil inside an MGW Lauda RC20 Model T-2 water bath (for recycled retentate/feed temperature control).

The pressure cell housed a test-tube shaped supported membrane. Cajon fittings allowed a rubber 'O'-ring to be compressed against both the supported membrane and the housing. The fittings resulted in a pressure-tight isolation of the feed (high pressure) and permeate (low pressure) streams.

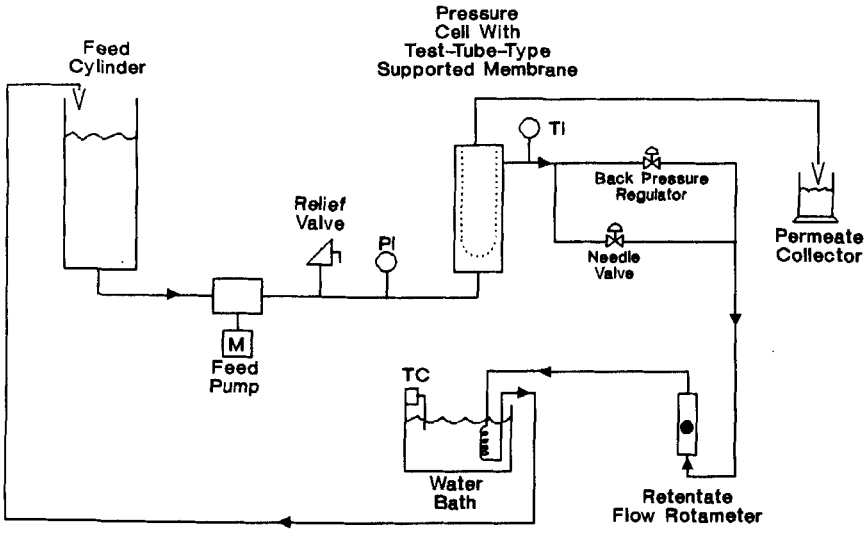

Figure 2. Schematic diagram of permeability test apparatus.

RESULTS AND DISCUSSION

Electron Microscopy Studies

A scanning electron photomicrograph of the top surface of a typical unsupported Al_2O_3 membrane is shown in Figure 3a. Dimples or craters which form during the drying process as water evaporates act as regions of stress concentration with potential adverse effects on the properties of the ultimate membrane. However, when the sol is slipcast onto a porous support, a more homogeneous membrane with no dimples is formed (see Figure 3b). The surface irregularities in Figure 3b are due to the rough surface of the underlying clay support, not the membrane. Apparently the driving force and the mechanism for solvent removal during slipcasting to prepare supported membranes are sufficiently different from those involved in preparing unsupported membranes to prevent dimples and craters from forming. In the former case water is absorbed into the pores of the support by capillary action, while in the latter case the water is evaporated over a period of 8-10 days. Both our work and results obtained by other workers (13) indicate that supports may alter surface aggregation processes.

Electron photomicrographs of typical fracture edges of unsupported Al_2O_3 membranes are shown in Figure 4. These photographs

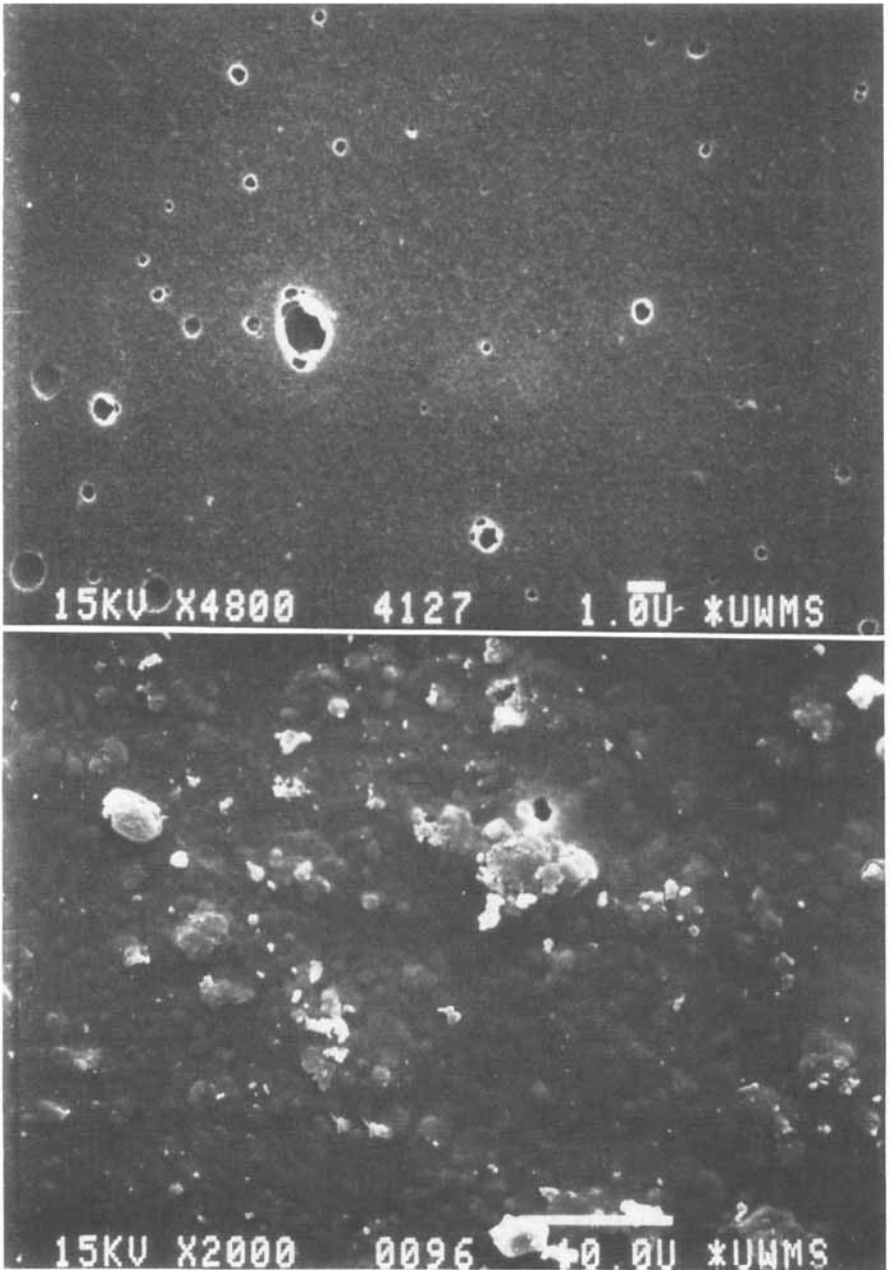

Figure 3. Photomicrographs of surface of unsupported alumina membrane.
a. magnification 4800.
b. magnification 2000.

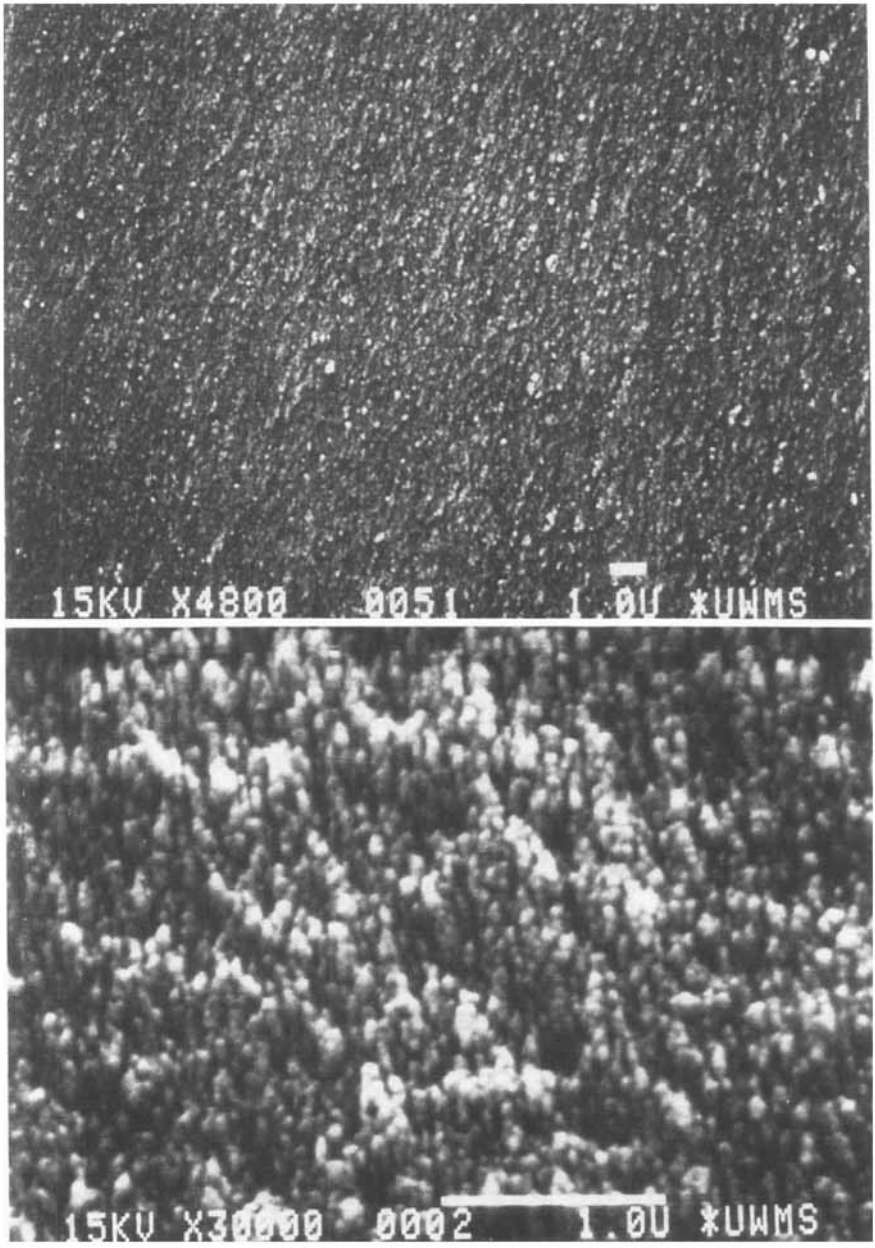

a

b

Figure 4. Photomicrographs of fracture edge of unsupported alumina membrane.
a. magnification 4800.
b. magnification 30000.

show no voids or defect structures in the bulk membrane. They indicate a reasonably constant particle size (ca. 50 nm) and shape. This result is in excellent agreement with an independent determination of particle size in the precursor sol by photon correlation spectroscopy. Although one cannot definitively conclude that these particles are either aggregates or primary particles, the agreement in size between these two alternative measurements indicates that the particles imaged in microscopy are the same as those measured in the precursor suspension after sonication for 20 minutes.

We have also obtained scanning electron photomicrographs of supported Al_2O_3 membranes after they have been used to ultrafilter test solutions. Figure 5a is a perpendicular view of the support used for the alumina membranes. Based on this and other photomicrographs, the effective pore size of the support appears to be about a micron. It should be noted that, in general, coverage of the support surface by the ceramic membrane is quite complete in spite of the high degree of irregularity of the underlying surface. The high degree of coverage can be seen in the cross-sectional view shown in Figure 5b. (In this case the support had been dipped into the sol and air dried four times prior to calcination at 500 C.) Another perspective on the extent of the coverage by the membrane is indicated in Figures 6a and 6b. Photomicrograph 6b is a close-up of the center portion of Figure 6a. In Figure 6b the lower right portion appears to be uncoated clay. Incomplete coverage of the support by the membrane would explain the fact that the supported membrane destroyed to obtain these photomicrographs exhibited unusually high permeation rates compared to other membranes prepared in a similar fashion.

Scanning electron photomicrographs were also obtained for TiO_2 membranes, both supported and unsupported. Good coverages of the support were obtained, although significant cracking and macropore formation were noted. Perpendicular views are shown in Figures 7a and 7b. The latter photomicrograph is that of a cracked edge, indicating the titania surface and the underlying clay support.

Sorption and Pore Size Distribution Measurements

BET adsorption measurements were carried out for a variety of unsupported membranes. Nitrogen was used as the adsorbate in all instances. Typical data are shown in Figure 8. These data correspond to a boehmite xerogel precursor and the unsupported ceramic membrane formed by firing the xerogel at 500 C for 24 hours. Equivalent results are obtained after only 1 hour at 500 C. Conventional BET calculations lead to the associated pore size distributions shown in Figures 8c and 8d. The gel exhibits primarily microporosity. Heating to 500 C enlarges the pores to an approximate modal size of 4 nm. This increase is not unex-

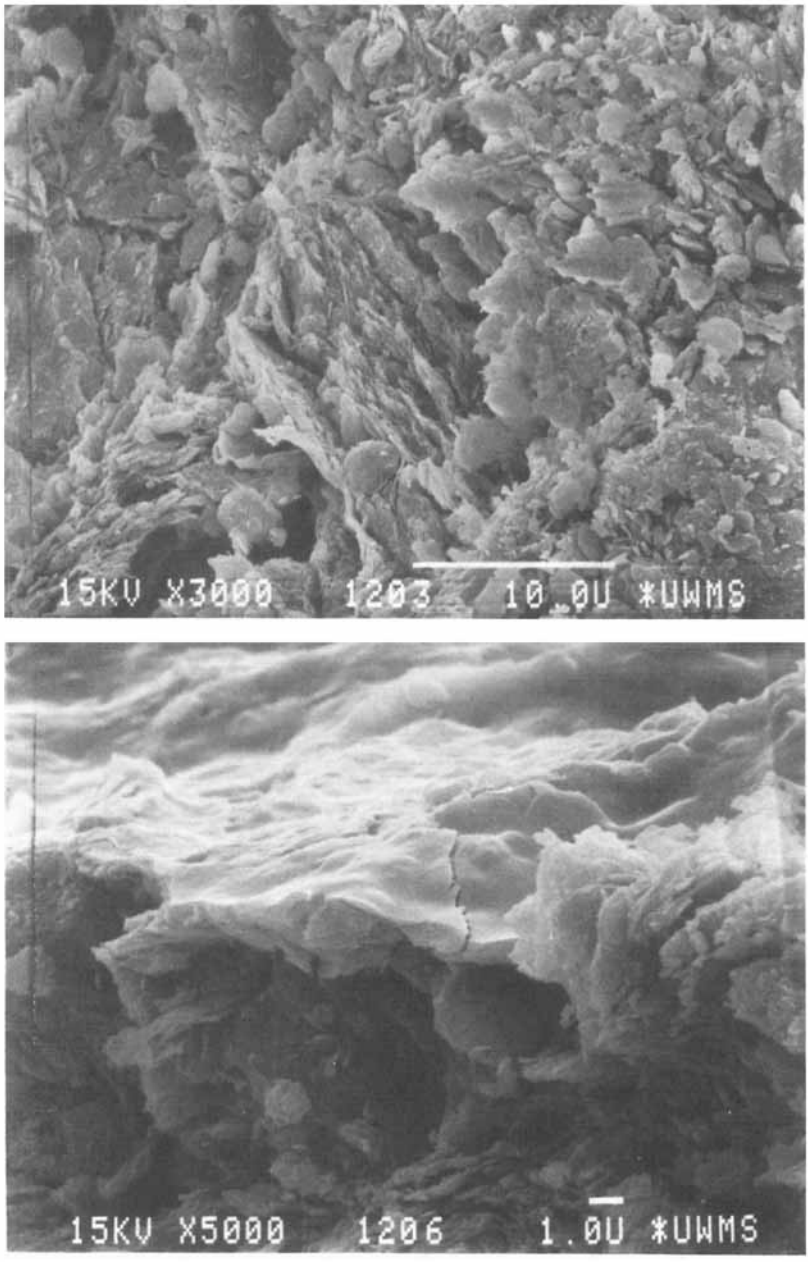

a

b

Figure 5. Photomicrographs depicting coverage of clay support by Al_2O_3 membrane.
a. Perpendicular view of clay support (x3000).
b. Cross section view of membrane and support (x5000).

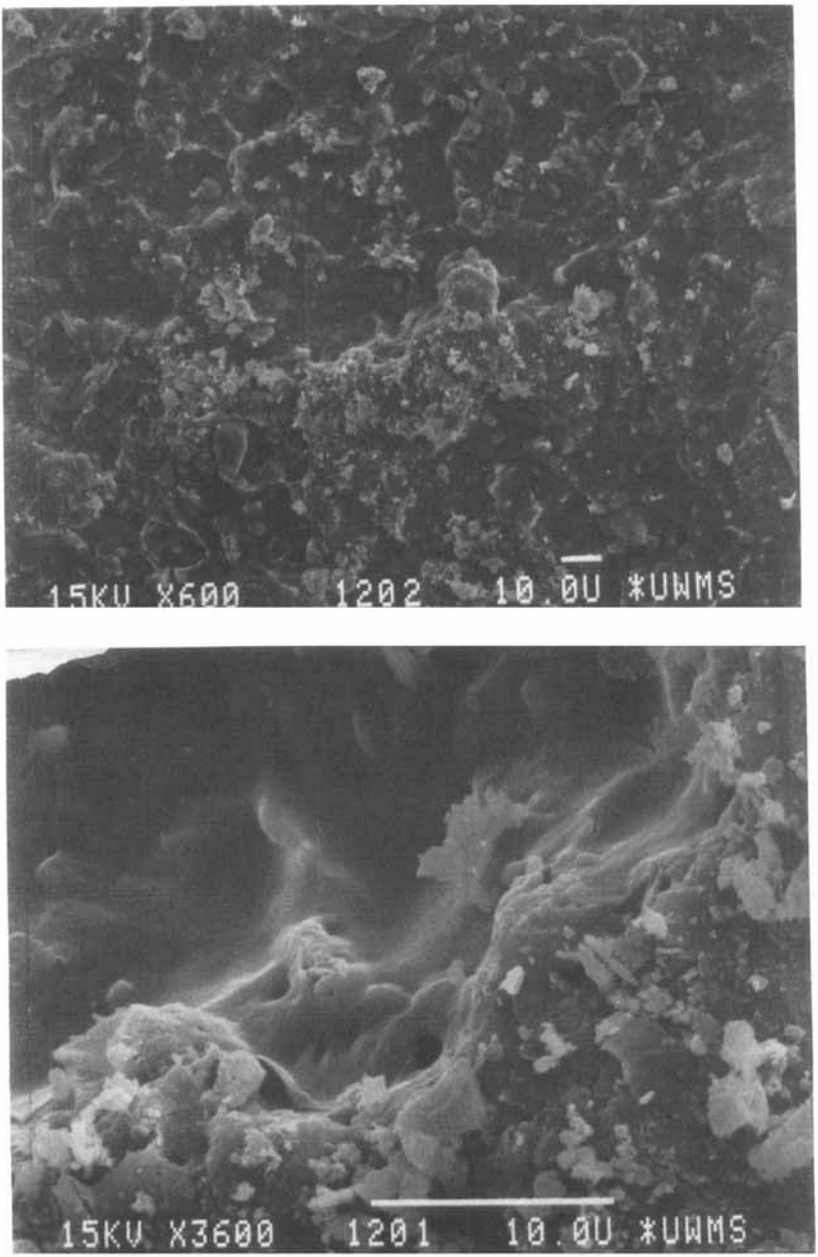

a

b

Figure 6. Perpendicular view of Al_2O_3 membrane dipped 4 times.
a. magnification 600.
b. magnification 3600.

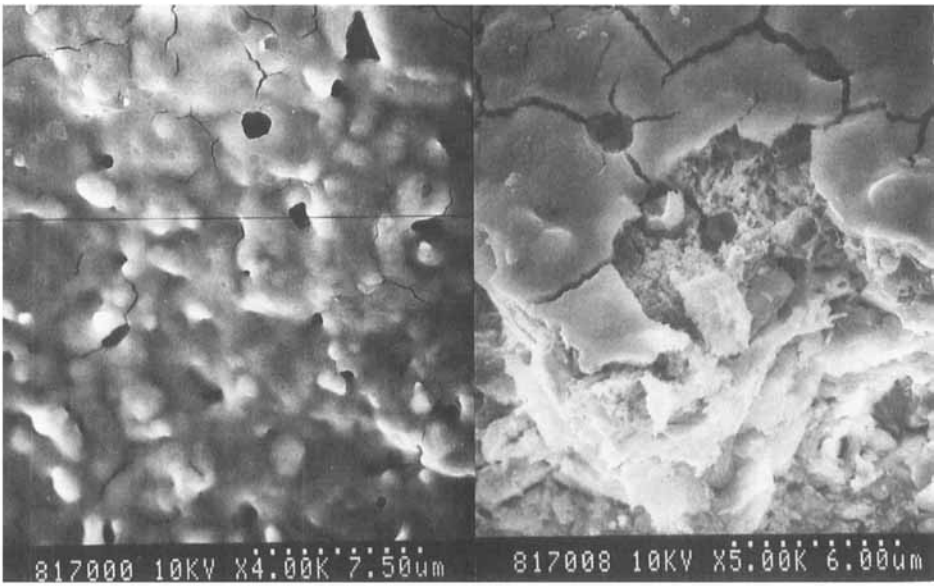

a. b.

Figure 7. Electron photomicrographs of supported TiO_2 membranes.
a. Perpendicular view (x4000).
b. Perpendicular view of cracked edge (x5000)

pected because this material undergoes a calcination reaction, but no real sintering or densification occurs at this temperature. Mercury porosimetry measurements on a membrane prepared from a sol of a similar composition gave a modal pore size of about 4.5 nm (14), a result which is in very good agreement with our findings.

The pore size distributions shown in Figure 8 were performed on the adsorption branch of the isotherm. Figure 9 shows the pore size distributions resulting from both the adsorption and desorption branches of the nitrogen isotherm. The sample is the Al_2O_3 ceramic shown in Figures 8b and 8d. Distributions from desorption branches are always much narrower than those from adsorption branches; the former emphasizes the neck or narrow regions of the pore structure whereas the latter more properly characterizes the overall morphology of the pore structure. In cases where a sieving mechanism is responsible for the permselectivity of

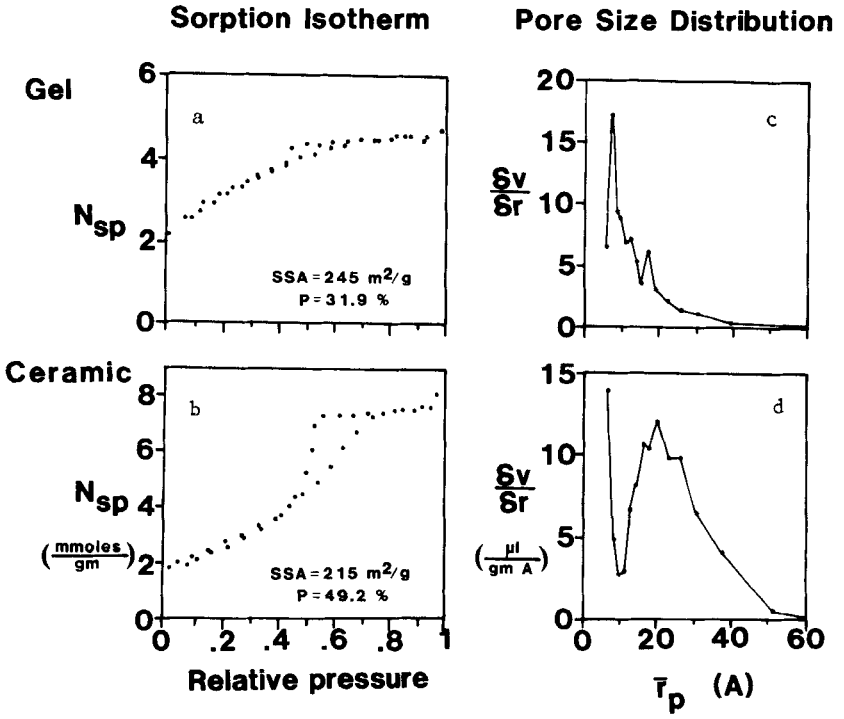

Figure 8. Adsorption isotherm (N_2) and pore size distribution data for xerogel precursor and sintered unsupported alumina membrane.

membranes, it is desirable to characterize both branches of the isotherm. The desorption branch characterizes the "bottlenecks" while the adsorption branch provides useful information for those systems where there are wide variations in the cross sectional area of the pore along its length.

Figure 10 illustrates the effect of variations of the initial HNO_3 to total aluminum ratios in the precursor solution on the pore structure of an unsupported Al_2O_3 membrane fired at 500 C. The data in Figure 10a were obtained from the sample prepared with the least amount of acid that could be used to obtain a stable sol. This sample had a very good total porosity (58%), but its pore size distribution was very broad and the gel cracked while drying. When more acid was added, membranes which remained intact during drying were produced. These membranes exhibited somewhat

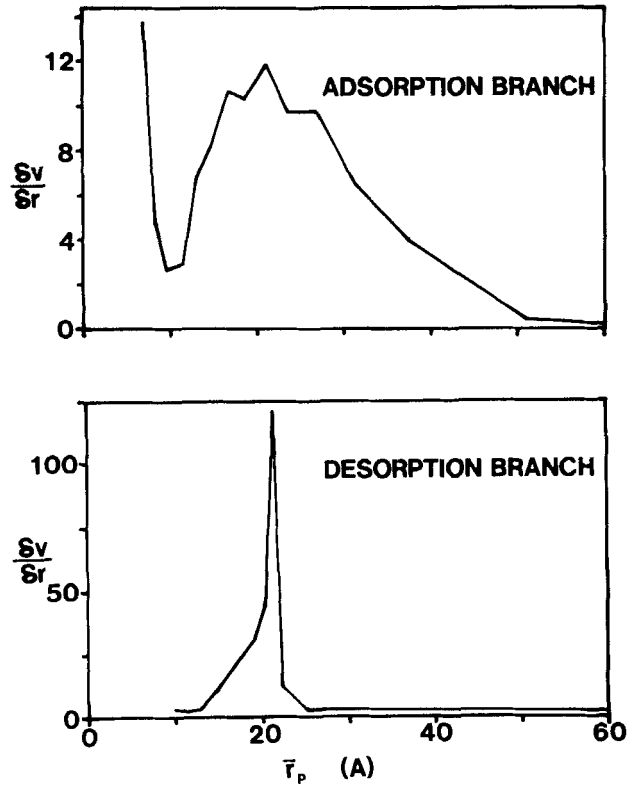

Figure 9. Pore size distributions corresponding to the adsorption and desorption branches of an adsorption isotherm (N_2) for an alumina membrane.

narrower pore size distributions, yet retained good porosities (ca. 50%).

Figure 11 indicates the effect of increasing the concentration of the inert electrolyte $NaNO_3$ from 0 to 0.1 M. The pore size distributions of the first three samples are very similar to one another. These gels formed crack free membranes which had porosities of about 50%. For sample 11d the pore size distribution broadened considerably and the total porosity is only 17%. This gel also cracked while drying.

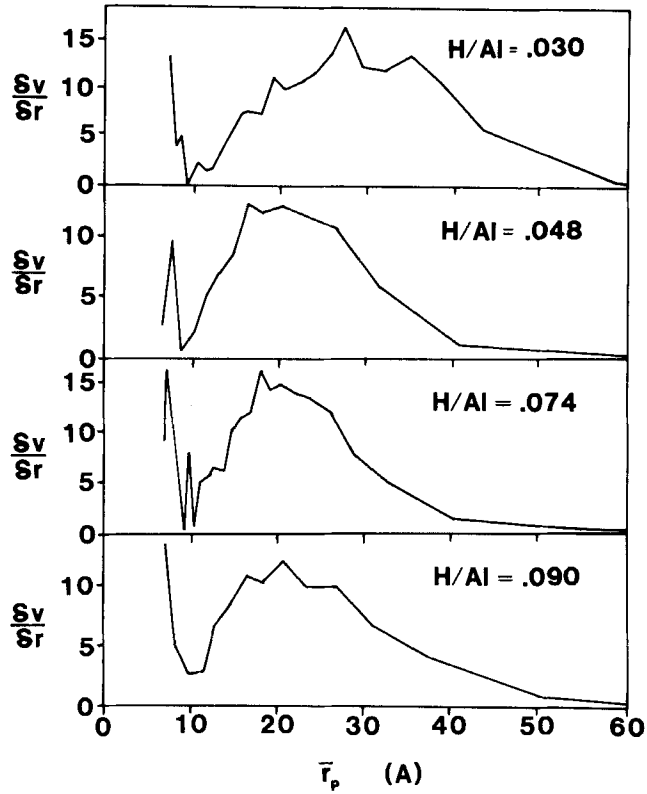

Figure 10. Effect of molar ratio of HNO_3 to total aluminum on the pore size distribution of an unsupported alumina membrane.

Combinations of phosphoric and nitric acid were utilized in another series of hydrolyses. The nitric acid served to peptize the sol particles while the phosphoric acid was added to determine its effect on the pore size distribution via potential enhancement of the degree of ordering of the particles. Anderson et al. (15) have shown that phosphoric acid forms bridges between goethite (α-FeOOH) particles and increases the crystalline order in the resultant aggregates. However, the pore size distributions of the membranes in question were very similar. All of these gels remained intact and had porosities of about 50%. While the BET results indicate that, in concentrations up to 10^{-3}M, phosphate additions did not seem to have any significant effect, they do not

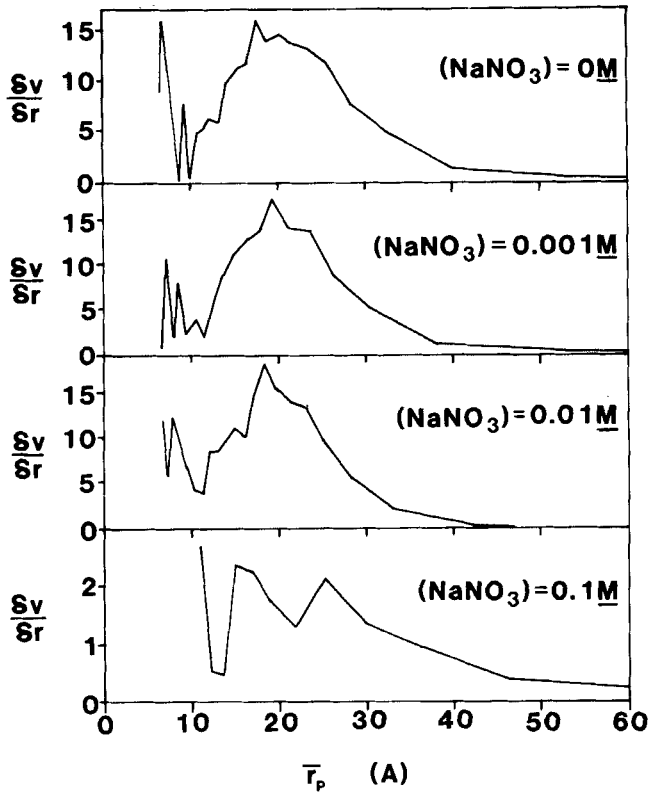

Figure 11. Effect of inert electrolyte concentration on the pore size distribution of an unsupported alumina membrane.

necessarily rule out the possibility that at higher concentrations phosphate may cause ordering and/or affect the final pore size distribution. Further experiments are planned in this area.

The effect of sintering temperature on the pore size distribution of Al_2O_3 membranes is depicted in Figure 12. If the sintering temperature is raised from 500 to 800 C the porosity of the Al_2O_3 membranes remains substantially constant at about 50%, but the pore size distribution broadens significantly with the modal pore size increasing from ca. 4.0 to ca. 7.5 nm. At the same time the specific surface area decreased from 260 to 150 m^2/g.

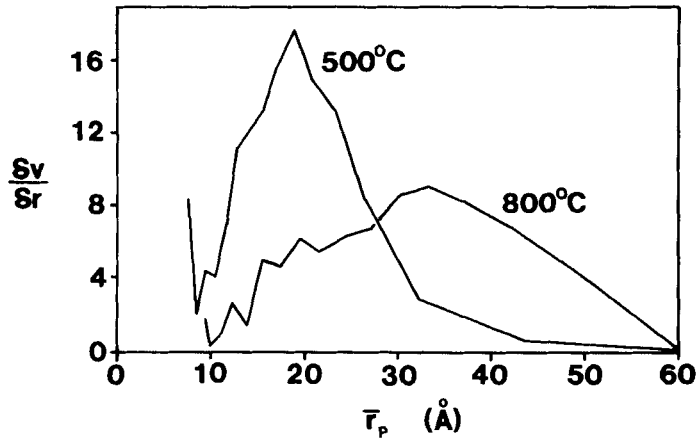

Figure 12. Effect of sintering temperature on the mean pore size and the pore size distribution of an unsupported alumina membrane.

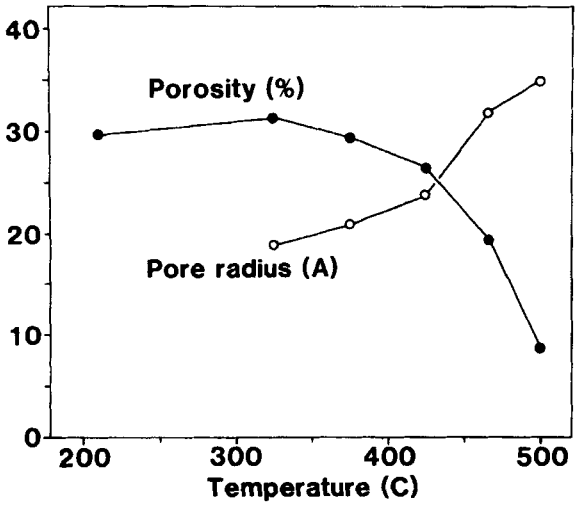

Figure 13. Effect of sintering temperature on the mean pore size and the porosity of an unsupported titania membrane.

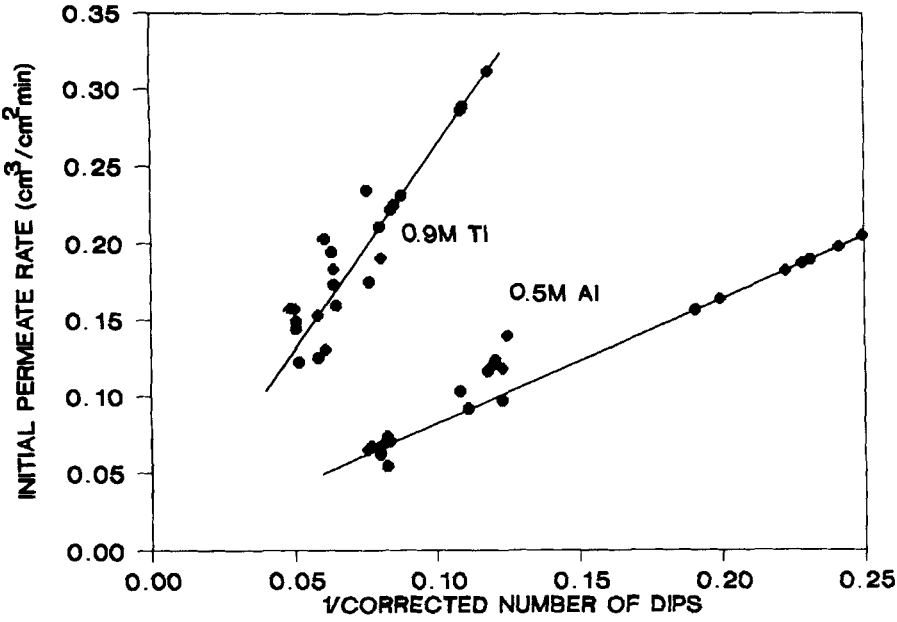

Figure 14. Permeate flux data at 100 psig and 25 C for supported alumina and titania membranes.

An increase in sintering temperature also broadens the pore size distribution of the titania membranes. The effect of temperature on the mean pore size and on the porosity of unsupported TiO_2 membranes is shown in Figure 13. Unlike the situation for the Al_2O_3 membranes, the porosity of the TiO_2 membranes decreases significantly as the sintering temperature is increased. In both cases, however, the mean pore size increases with increasing temperature.

Permselectivity Measurements

Permeation rate and rejection measurements were conducted for a series of supported Al_2O_3 and TiO_2 membranes of various thicknesses. The sols used to prepare the membranes had the following compositions:

Alumina Sol	Titania Sol
0.5M Total Al	0.278M Total Ti
0.035M NO_3^-	0.111M NO_3^-
10^{-5}M H_3PO_4	
pH 3.9-4.0	pH 1.3

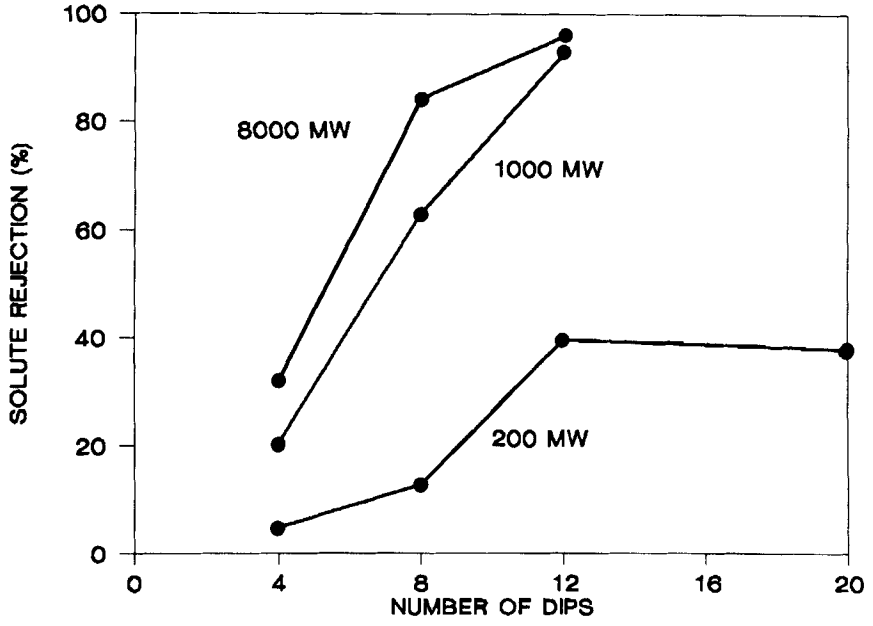

Figure 15. Rejection of polyethylene glycols by supported alumina membranes.

The water soaked supports were dipped into the sols and dried using the procedure shown in Figure 1. They were fired after every fourth dip in order to fix the membrane for the permselectivity tests. Electron photomicrographs of the resulting supported membranes suggested that these four dips into the sol ultimately led to membranes with total thicknesses of ca. 1.0 and 0.6 microns for alumina and titania, respectively.

Evidence that these systems behaved linearly with respect to the number of dips was provided by checking the permeability of the supported membranes to pure water. For a conventional membrane transport model the permeation rate of a solvent should be inversely related to the thickness of the membrane. If the increment in membrane thickness formed by each dip is uniform, the permeate flux should be inversely related to the number of dips. Since the total resistance to transport through the supported membrane consists of two contributions - that due to the support and that due to the membrane proper - appropriate experiments can generate the data necessary to determine the equivalent resistance of the support. If one carries out measurements of this type, it

is possible to create a plot of permeate flux versus the reciprocal of the number of dips corrected for the contribution of the support to the overall resistance (see Figure 14). Such a plot indicates that the titania membrane is clearly much more permeable to water than is the alumina membrane, even allowing for the differences in the concentrations of the precursor sols employed in the preparation of these membranes.

To determine the rejection characteristics of the supported membranes, aqueous solutions of polyethylene glycol (1% w/w, molecular weights of 200, 1,000, and 8,000) were employed. The test loop was operated with total recycle of retentate and permeate so as to maintain a constant composition of the feed stream. Solute rejections were calculated as

$$\text{Percent Rejection} = 100(1-[C_{permeate}/C_{feed}])$$

The results of the experiments for the supported alumina membranes are summarized in Figure 15. The rejection increases with increasing molecular weight, as one would expect. Rejection also increases with increasing thickness of the membrane, at least to a point. (It was not possible to obtain more than 40% rejection of the polyethylene glycol with a molecular weight of 200 even using membranes which had been dipped a large number of times.)

Preliminary measurements of rejection coefficients for polyethylene glycol with a molecular weight of 8,000 indicated that the supported TiO_2 membranes were not at all selective (i.e., the rejection coefficients were only 1-3%). Consequently aqueous solutions of bovine serum albumin were used as test solutions. In this case rejection coefficients in the 87-97% range were observed. Failure to achieve complete rejection of the albumin can be attributed to the possible presence of cracks and/or macropores in the surface of the titania membrane.

SUMMARY:

Electron microscopy, BET adsorption, and permselectivity measurements were used to characterize supported and unsupported TiO_2 and Al_2O_3 membranes. Such measurements can be used in the optimization of membrane preparation procedures so as to produce membranes which have the desired morphological and permselectivity characteristics. We have been able to produce membranes with pore diameters in the 35-50 Angstrom range. Our initial results look very promising in that we have been able to obtain very good solute rejection with reasonable flow rates. Further work on supported alumina and titania membranes is in progress with the long range goal of linking modifications in the surface and colloid chemistry of the precursor sols to their concomitant effects on the permselectivity characteristics of the finished membranes.

ACKNOWLEDGEMENTS:

The authors gratefully acknowledge the financial support of the Department of Energy - Office of Industrial Programs under Contract Number DE-AS07-86ID12626. We would also like to acknowledge the assistance of Brian Bischoff in this work.

REFERENCES:

1. Barringer, E. A., and H. K. Bowen, Langmuir, 1, 414 (1985).

2. Yoldas, B. E., Am. Cer. Soc. Bull., 54, 296 (1975).

3. Yoldas, B. E., J. Mater. Sci., 10, 1856 (1975).

4. Kaiser, A., and H. Schmidt, J. Non-Cryst. Solids, 63, 261 (1984).

5. Leenaars, A. F. M., K. Keizer and A. J. Burggraaf, J. Mater. Sci., 19, 1077 (1984).

6. Leenaars, A. F. M., and A. J. Burggraaf, J. Membrane Sci., 24, 261 (1985).

7. Leenaars, A. F. M., K. Keizer and A. J. Burggraaf, paper presented at the ACS Symposium on Reverse Osmosis and Ultrafiltration, August 26-31, 1984, Philadelphia, Pennsylvania. To be published in ACS Symp. Ser., S. Sourirajan (Ed.).

8. Keizer, K., A. F. M. Leenaars and A. J. Burggraaf, Sci. of Ceram., 12, 101 (1984).

9. Yoldas, B. E., and T. W. O'Keefe, Appl. Opt., 18, 3133 (1979).

10. Dislich, H., and P. Hinz, J. Non-Cryst. Solids, 48, 11 (1982).

11. Brinker, C. J., and M. S. Harrington, Sol. Energy Mater., 5, 159 (1981).

12. Anderson, M. A., M. J. Gieselmann and Q. Xu, accepted for publication in J. Membrane Sci.

13. Livage, J., J. Solid State Chem., 64, 322 (1986).

14. Shafer, M. W., personal communication, 1987.

15. Anderson, M. A., M. I. Tejedor-Tejedor and R. R. Stanforth, Environ. Sci. Technol., 19, 632 (1985).